The Journal of Chemical Physics ARTICLE scitation.org/journal/jcp

Internal dynamics of methyl *p*-tolyl sulfoxide in the gas phase: Rotational spectroscopy and theoretical studies

Cite as: J. Chem. Phys. 156, 000000 (2022); doi: 10.1063/5.0083534
Submitted: 27 December 2021 • Accepted: 2 March 2022 •
Published Online: 9 99 9999

View Online Export Citation CrossMark

Wenhao Sun,[1,a)] Isabelle Kleiner,[2] Arne Senftleben,[3] and Melanie Schnell[1,4,a)]

AFFILIATIONS

[1] Deutsches Elektronen-Synchrotron DESY, Notkestraße 85, 22607 Hamburg, Germany
[2] Laboratoire Interuniversitaire des Systèmes Atmosphériques (LISA), CNRS UMR 7583, Université de Paris, Université Paris-Est Créteil, Institut Pierre Simon Laplace, 61 Avenue du Général de Gaulle, 94010 Créteil, France
[3] Universität Kassel, Heinrich-Plett-Str. 40, 34132 Kassel, Germany
[4] Institute of Physical Chemistry, Christian-Albrechts-Universität zu Kiel, Max-Eyth-Straße 1, 24118 Kiel, Germany

[a)] **Authors to whom correspondence should be addressed:** wenhao.sun@desy.de and melanie.schnell@desy.de

ABSTRACT

A pure rotational spectrum of methyl *p*-tolyl sulfoxide (MTSO) was studied using chirped-pulse Fourier transform microwave spectroscopy in the frequency range of 18–26 GHz. A single conformer was unambiguously observed in the supersonic jet expansion, which is consistent with the conformational analysis performed using quantum-chemical calculations. Rotational transitions were split into two components of *A* and *E* symmetries due to the low-barrier internal rotation of the ring methyl group [V_3 = 11.0178(23) cm^{-1}]. The low energy barrier for the methyl top internal rotation implies an electron-withdrawing effect of the group at the opposite side of the phenyl ring, in comparison with other *para*-substituted toluenes. The effective ground state (r_0) geometry was derived using the rotational constants from the parent species and the ^{34}S and eight ^{13}C singly substituted isotopologues. Compared to two other sulfoxides, methyl phenyl sulfoxide and methyl 4-nitrophenyl sulfoxide, the sulfoxide group in MTSO is slightly more twisted with respect to the plane of the phenyl ring, which could be attributed to the moderate electron-donating effect of the *p*-methyl group. Furthermore, the pyramidal inversion that interconverts the handedness at the sulfur stereogenic center was explored in the electronic ground (S_0) and excited (S_1) states with nudged elastic band and time-dependent density functional theory methods. It was found that the pyramidal inversion in S_1 is easier than in S_0, showing that optical excitation to S_1 will facilitate an effectively barrier-free inversion.

I. INTRODUCTION

Structural flexibility is a key feature for many molecules, including chiral ones, and it finds application in different areas of chemical and biochemical processes, such as improved interactions due to structural rearrangements in molecular recognition.[1] Structural flexibility of chiral molecules can, however, also be of great relevance for advanced molecular physics experiments, aiming at controlling and manipulating chirality at the molecular level in the gas phase. Of particular interest here are intramolecular motions that change the handedness of a molecule, such as in HOOH,[2] biphenyls,[3] sulfoxides,[4] and structurally related molecules, where the enantiomers can rapidly interconvert via tunneling. Such tunneling motions are central for an experimental proposal to determine the small energy difference between the two enantiomers due to the parity-violating effect of the weak interaction, for example.[5] Likewise, large-amplitude/vibrational motions can induce chirality, such as in small carbonyl-containing molecules (such as COFCl)[6] or carbonic acids, such as formic acid.[7]

Another class of chiral molecules showing structural flexibility is asymmetrically substituted sulfoxides, such as methyl phenyl sulfoxide (MPS)[8] and methyl 4-nitrophenyl sulfoxide (MNPSO).[9] In their electronic ground states, the sulfoxide group adopts a pyramidal configuration. As such, these molecules are chiral with stable enantiomers, i.e., separated by a high barrier so that they do not interconvert on any relevant time scale. Upon electronic excitation,

however, the sulfoxide group may become planar, resulting in an achiral species, or become near-planar with the inversion barrier significantly reduced.[10] This property is of interest for experiments that aim at transferring molecules of one handedness into the other handedness using optimized light pulses and well-controlled samples in the gas phase.[11,12] For these experiments to be possible, however, a detailed understanding of the structure and intramolecular dynamics of these molecules isolated in the gas phase is necessary.

Rotational spectroscopy is an established technique to obtain precise molecular structures of gas-phase molecules.[13] Rotational transition frequencies are inherently linked to the molecular structure via the moments of inertia. Experimental bond lengths and angles can be obtained through isotopic substitution, observed either in natural abundance or in enriched samples. Isotopic substitution changes the mass distribution of the molecules and, thus, the moments of inertia, which can be resolved in the rotational spectra. In turn, different spectra for singly substituted isotopologues can be used to determine the positions of the atoms in a molecule or a molecular complex with respect to the center of mass of the species. Intramolecular dynamics can result in characteristic splittings of rotational transitions, and their analysis gives reliable information of the respective motion and their associated barriers.[14] These information can provide insights into the chemical and physical properties of this molecule.

In the present work, we investigate methyl *p*-tolyl sulfoxide (MTSO) using broadband rotational spectroscopy to obtain its structure, with a particular focus on the arrangement of the sulfoxide group. The observed torsional splittings arising from the ring methyl group, which give information on the electron-withdrawing effect of the sulfoxide group, are carefully analyzed. A comparison with related sulfoxides, such as methyl phenyl sulfoxide, is particularly interesting, for example, to shed light on the effect of the *para*-substituents on the geometry of the sulfoxide group and the pyramidal inversion dynamics. The spectroscopy work is accompanied by quantum-chemical calculations at the density functional level of theory.

II. EXPERIMENTAL DETAILS

The pure rotational spectrum of methyl *p*-tolyl sulfoxide was collected using our segmented 18–26 GHz chirped-pulse Fourier transform microwave (CP-FTMW) spectrometer.[15] The compound [97% chemical purity, melting point (mp): 44–46 °C] was purchased from Sigma-Aldrich and used without further purification. In order to obtain a sufficient vapor pressure, the solid sample was placed in a heatable nozzle reservoir and maintained at 100 °C. The vapor was carried by a neon buffer gas with a stagnation pressure of ~3 bars and seeded into a supersonic expansion through a solenoid valve (Parker General Valve, Series 9) pulsing at 10 Hz. Following the expansion of each gas pulse, a series of three pulse trains, which covers the entire bandwidth of 8 GHz by combining ten 800 MHz segments, was used to polarize the ensemble of the molecules. Afterward, 10 μs of the free induction decay (FID) were recorded in the time domain for each segment. More details of the segmented approach can be found in Ref. 15. In total, 2.1 $\times 10^6$ FIDs were measured and averaged for each segment and combined together in the frequency domain after fast Fourier transformation. The spectral resolution based on the digitization rate of the Keysight digitizer card (3.2 GS/s) is 100 kHz, and the typical FWHM linewidths are ~200 kHz after applying the Kaiser–Bessel window function.

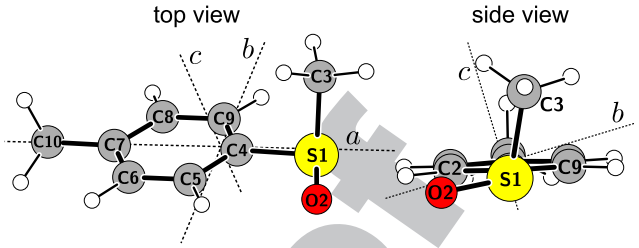

FIG. 1. The equilibrium structure of methyl *p*-tolyl sulfoxide (MTSO) in the principal axis system as obtained from the B3LYP-D4/def2-QZVP geometry optimization.

III. COMPUTATIONAL DETAILS

The quantum-chemical calculations were carried out using the ORCA 4.2.1 program.[16,17] The geometry of MTSO was optimized using the density functional theory (DFT) B3LYP method[18–20] in combination with Grimme's D4 dispersion correction[21] and the Karlsruhe def2-QZVP basis set.[22] The obtained equilibrium structure is shown in Fig. 1, and the corresponding rotational constants and electric dipole moment components were used for further spectral assignments. To investigate the large-amplitude motions of the two methyl groups, i.e., the sulfoxide and ring methyl groups, potential energy scans were performed by rotating them around the S_1–C_3 and C_7–C_{10} bonds, respectively, in 10° steps from −180° to 180°. These calculations were carried out at the same level of theory as the structural optimization, while all other geometrical parameters were relaxed. As the V_3 torsional barrier of the ring methyl group is relatively low (~10 cm^{-1}), more accurate DFT integration grids for SCF iterations (Grid5) and final energy evaluations (Grid6) were used instead of the default settings (Grid2 and Grid4) to achieve higher precision.[23]

As mentioned earlier, the stereomutation at the stereogenic sulfur atom, which adopts a trigonal pyramidal configuration, is of important concern. Nudged Elastic Band (NEB) calculations[24] were, therefore, performed for MTSO and other relevant sulfoxides to explore the minimum energy path and search for the transition state of the pyramidal inversion in the electronic ground state (S_0). The located saddle point connecting the enantiomer pair of the global minimum was fully re-optimized to obtain the transition state. Furthermore, the time-dependent (TD) B3LYP method[25] with the def2-QZVP basis set and the Resolution of Identity (RI) approximation was exploited to compute the electronic transitions and to optimize the geometries of both the equilibrium state and the inversion transition state in the first electronic excited state (S_1). The orbital analysis was performed with the Multiwfn program.[26]

IV. RESULTS AND DISCUSSIONS

A. Spectral assignments and fits

The torsional energy curves of the internal rotation motions are shown in Fig. 2, and the threefold internal rotation barrier (V_3) is calculated to be 11.6 kJ/mol (965 cm^{-1}) for the sulfoxide methyl

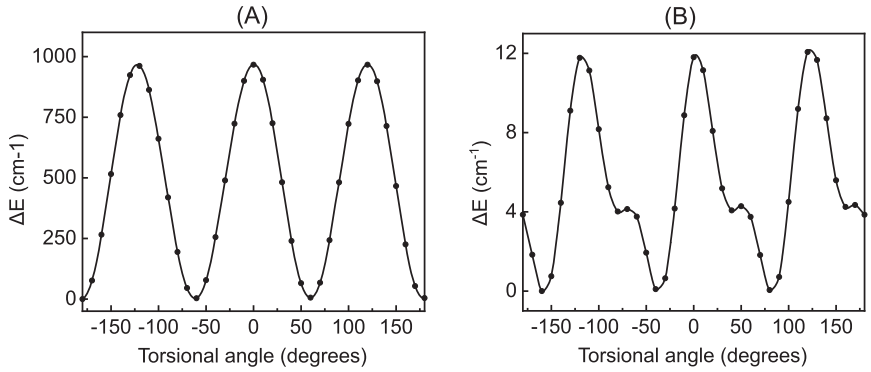

FIG. 2. (a) The potential energy curve (PEC) obtained by rotating the sulfoxide methyl group around the S_1–C_3 bond at the B3LYP-D4/def2-QZVP level of theory. (b) The PEC obtained by rotating the *p*-methyl group around the C_7–C_{10} bond.

group and 0.14 kJ/mol (11.7 cm^{-1}) for the *p*-methyl group, respectively. The shoulder in Fig. 2(b), which shows the internal rotation of the *p*-methyl group, is due to the moderately distorted phenyl ring by the methylsulfinyl group. Such a low barrier of the ring methyl group has been explored in other *para*-substituted toluenes and will be discussed in Sec. IV B. Experimentally, only splittings arising from the torsion of the *p*-methyl group are resolved in the spectrum (see Fig. 3). At the first stage, 127 spectral lines corresponding to the *A* tunneling states were readily assigned, including all three types of transitions, which is consistent with the calculated electric dipole moment components from the DFT calculations (μ_a = 2.9 D, μ_b = 2.8 D, and μ_c = 1.3 D). These collected transitions were fitted with Pickett's SPFIT program[27] using Watson's *A*-reduced Hamiltonian in the I^r representation, which gave a root-mean-square deviation (RMSD) of 5.8 kHz.[28]

Next, the fit of *A* species was transferred to the XIAM program.[29] The transitions corresponding to the *E* torsional state were identified in the spectrum and gradually included to obtain a global fit. The splittings of *a*-type transitions are relatively small (within 150 MHz), while *b*- and *c*-types show much larger splittings of up to 2 GHz. Regarding the intensities of the *A*/*E* components, their intensity ratios depend not only on the magnitude of the dipole moment components (μ_a, μ_b, and μ_c) but also on the mixing of the wavefunctions within the eigenvectors describing the initial and final states of the transition, as shown in Ref. 30 after Eq. (15). For *a*-type transitions, the intensity ratios of the splittings are about 1:1, as shown in Fig. S1 of the supplementary material. However, they are different for *b*- and *c*-type transitions. In the spectrum, the *E* components of *c*-type transitions are more intense than their *A* components, as presented in the zoomed-in panel of Fig. 3. On the contrary,

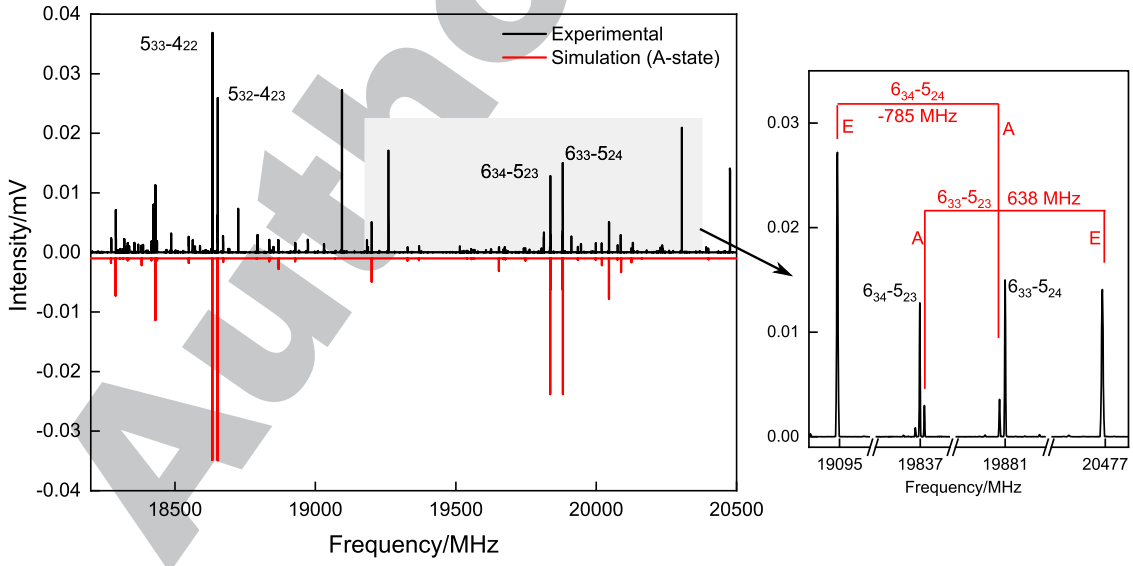

FIG. 3. Section of the microwave spectrum of methyl *p*-tolyl sulfoxide (MTSO) from 18 to 20.5 GHz resulting from an accumulation of 2.1 ×10^6 FIDs. In the left panel, the experimental spectrum (in black) is shown in the upper trace and the simulated spectrum of *A* species (in red) based on the SPFIT results, as given in Table I, is shown in the bottom trace. In the right panel, the *A*/*E* splittings are highlighted for two *c*-type transitions. The splittings are 638 and −785 MHz for the 6_{33}–5_{23} and 6_{34}–5_{24} transitions, respectively. The corresponding observed intensity ratios of *A*/*E* *c*-type transitions are 1:5 and 1:8. In contrast, the *E* components of the 6_{34}–5_{23} and 6_{33}–5_{24} transitions are not observed as they lack of sufficient strength.

TABLE I. Molecular constants in the principal axis system (PAM) for the parent isotopologue of methyl *p*-tolyl sulfoxide (MTSO) obtained with the BELGI-C_1, XIAM, and SPFIT codes in comparison to the results calculated at the B3LYP-D4/def2-QZVP level of theory.[a]

Parameter[b]	Unit	Prediction[c]	BELGI-C_1	XIAM	SPFIT
A	MHz	3071.94	3062.414 2(66)[d]	3060.990(77)	3119.314 18(58)
B	MHz	638.42	641.401 47(56)[d]	641.506 0(13)	641.500 67(19)
C	MHz	576.04	577.243 89(55)[d]	577.344 9(14)	577.348 75(20)
Δ_J	kHz	⋯	⋯	0.042 2(25)	0.020 94(36)
Δ_{JK}	kHz	⋯	⋯	0.113(11)	0.111 2(13)
Δ_K	kHz	⋯	⋯	−1.948(93)	0.494(21)
δ_J	kHz	⋯	⋯	0.001 80(74)	0.000 809(73)
δ_K	kHz	⋯	⋯	0.30(17)	0.239(17)
V_3	GHz	350.8	330.305(69)	345.7(17)	⋯
V_3	J/mol	140.0	131.802(28)	137.9(42)	⋯
V_3	cm^{-1}	11.7	11.017 8(23)	11.53(14)	⋯
F	GHz	⋯	162.503(23)	160.80[e]	⋯
F_0	GHz	161.90	159.436(39)	157.71(21)	⋯
I_α[f]	$\mu Å^2$	3.12	3.169 771 5(75)	3.204 5(43)	⋯
∠(i, a)	deg	5.13	5.957 543(99)	5.951 5(6)	⋯
∠(i, b)	deg	86.67	86.907 20(18)	84.920 6(10)	⋯
∠(i, c)	deg	93.90	95.086 880(39)	93.093 5(11)	⋯
μ_a	D	2.9	✓[g]	✓	✓
μ_b	D	2.8	✓[g]	✓	✓
μ_c	D	1.3	✓[g]	✓	✓
No. of lines	⋯	⋯	127(A) + 123(E)	127(A) + 123(E)	127(A)
rms	kHz	⋯	8.5	71.9	5.8

[a]The complete BELGI-C_1 and XIAM fits are provided in Tables S1 and S2, respectively, of the supplementary material.
[b]All parameters refer to the inertial principal axis system. For the centrifugal distortion constants, Watson's *A*-reduction and an I^r representation were used.
[c]Computed at the B3LYP-D4/def2-QZVP level of theory.
[d]Obtained by the transformation from the rho-axis system to principal axis system.
[e]Derived from the fitted parameter F_0.
[f]Moment of inertia I_α of the internal rotor, calculated from its rotational constant F_0.
[g]Types of transitions (*a*-, *b*-, or *c*-type) observed.

most of the *b*-type *E* transitions in this frequency range are too weak to be observed except the Q branch transitions, despite the fact that μ_b is larger than μ_c and their *A* components are intense. In total, 123 *E* state lines were included in the XIAM fit, which yielded a RMSD of 71.9 kHz. The line strengths predicted by XIAM are in good agreement with the experimental spectrum. Although the program XIAM is convenient to use, the result was not satisfactory due to the lack of higher order coupling terms between the internal rotation and the overall rotation. The fit was further refined using the BELGI-C_1 code,[31] and the RMSD was significantly reduced to 8.5 kHz. The complete results from the BELGI-C_1 and XIAM fits are given in Tables S1 and S2 (see the supplementary material), respectively. The common spectroscopic parameters from these two fits are compared in the principal axis system (PAM), after transforming the RAM parameters from BELGI-C_1 into the PAM system, as given in Table I, along with the results from the DFT calculations.

B. Internal rotation

The torsional barrier (V_3) of the ring *p*-methyl group in MTSO is 11.0178(23) cm^{-1} in the BELGI fit. Due to the fact that only ground state ($v_t = 0$) transitions were observed from the cold molecular beam, the contribution of V_6 cannot be assessed in the current fit.[33] The obtained V_3 potential is lower than the values determined for many other *para*-substituted toluenes, which include *p*-cresol [18.39(3) cm^{-1}],[34] 4-methylacetophenone [21.744 98(6) cm^{-1}],[35] *p*-tolualdehyde [28.111(1) cm^{-1}],[36] and *p*-methylanisole [49.6370(1) cm^{-1}].[37] Although *p*-toluic acid has a slightly lower V_3 potential [7.899(1) cm^{-1}], the leading term of its torsional potential, V_6 [−24.77(2) cm^{-1}], is three times greater.[38]

In previous studies, the height of the V_3 potential was intuitively correlated with the symmetry of the phenyl frame to which the *p*-methyl group is attached. The closer the frame to a C_{2v} symmetry, which resembles the phenyl ring in toluene, the lower the barrier of the V_3 potential.[37] This phenomenon can be further rationalized from the perspective of the substituent effects, as the only difference across the above-mentioned toluenes is the groups at the *para*-position.[39] Although these functional groups have no direct interaction with the methyl group at the opposite side, their electronic donating/withdrawing effects can influence the delocalized π cloud in the phenyl ring and, consequently, change the electron density in the vicinity of the *p*-methyl group. The lower the

TABLE II. Equilibrium state (r_e) (B3LYP-D4/def2-QZVP), effective ground state (r_0), and XRD crystal structural parameters (bond lengths in Å and angles in degrees) of methyl *p*-tolyl sulfoxide (MTSO).

Bonds	r_e	r_0	XRD[a]	Angles	r_e	r_0	XRD[a]
r(O_2–S_1)	1.486	1.487(9)	1.505	∠(C_3–S_1–O_2)	106.3	105.5(7)	105.5
r(C_3–S_1)	1.821	1.813(10)	1.809	∠(C_4–S_1–O_2)	107.4	106.5(5)	106.5
r(C_4–S_1)	1.804	1.800(8)	1.804	∠(C_4–S_1–C_3)	96.5	96.0(5)	97.6
r(C_5–C_4)	1.385	1.393(10)	1.380	∠(C_5–C_4–S_1)	118.9	119.0(5)	120.8
r(C_6–C_5)	1.389	1.400(8)	1.376	∠(C_6–C_5–C_4)	119.2	119.2(6)	120.1
r(C_7–C_6)	1.394	1.398(9)	1.396	∠(C_7–C_6–C_5)	121.3	120.8(6)	121.0
r(C_8–C_7)	1.396	1.406(9)	1.376	∠(C_8–C_7–C_6)	118.4	118.6(5)	118.2
r(C_9–C_8)	1.387	1.394(8)	1.393	∠(C_9–C_8–C_7)	121.0	121.2(5)	121.9
r(C_9–C_4)	1.389	1.388(9)	1.397	∠(C_4–C_9–C_8)	119.4	119.0(6)	118.5
r(C_{10}–C_7)	1.504	1.508(7)	1.518	∠(C_5–C_4–C_9)	120.7	121.3(6)	120.3
				∠(C_{10}–C_7–C_6)	120.9	120.9(6)	120.5
				τ(O_2–S_1–C_4–C_3)	109.4	108.2(8)	108.7
				τ(O_2–S_1–C_4–C_5)	7.2	6.7(15)[b]	8.2

[a]Data from Ref. 32. The uncertainties are 0.003–0.006 Å for bond lengths and 0.3° for angles.
[b]Due to the lowest vibrational motion (42 cm^{-1}), in which the S=O group moves toward the phenyl plane, the uncertainty for this dihedral angle is higher.

electron density, the lower the hindrance while rotating the methyl group and the lower the potential barrier and vice versa. It is known that the methoxy group (–OCH_3) and hydroxyl group (–OH) are electron-donating groups, while the acetyl group [–C(=O)CH_3], aldehyde group (–CH=O), and carboxyl group [–C(=O)OH] have opposite effects.[40] Therefore, *p*-methylanisole has a relatively high V_3 term compared to others. Despite the electron donation of the hydroxyl group, the potential barrier of *p*-cresol is lower than *p*-methylanisole and even slightly lower than those with electron-withdrawing groups. This can be attributed to the well-conserved symmetry in *p*-cresol. On the contrary, when it comes to MTSO, although the methyl sulfoxide group has the lowest symmetry among these toluenes, it has the lowest torsional potential due to the electron-withdrawing effect of the sulfoxide group.

C. Structural determination

Besides the normal species, spectra from the ^{34}S isotopologue and the eight singly substituted ^{13}C isotopologues were assigned in their natural abundances and fitted with the BELGI-C_1 program. The corresponding rotational constants are provided in Table S3 of the supplementary material. Afterward, the 30 rotational constants obtained from the set of ten isotopologues allow us to derive the effective ground state structure (r_0) by exploiting the STRFIT87 program of Schwendeman.[41]

The determined geometrical parameters of the MTSO backbone are summarized in Table II in comparison with the equilibrium geometry (r_e) calculated at the B3LYP-D4/def2-QZVP level of theory and the crystal structure previously determined by an x-ray diffraction study.[32] Overall, the results obtained from the present gas-phase experiment show a better agreement with the theoretical structure, compared to that from the crystal XRD study, which can be attributed to crystal effects. The overlap of the experimentally derived heavy-atom positions with the optimized geometry is depicted in Fig. 4.

According to the obtained structure, the sulfoxide moiety (–S=O) is arranged almost co-planar with the phenyl plane. The twist angle, τ(O_2–S_1–C_4–C_5), is determined to be 6.7(15)°. The adjacent methyl group is almost perpendicular to the ring plane with a dihedral angle, τ(O_2–S_1–C_4–C_3), of 108.2(8)°. The orientation of the sulfoxide group favors the overlap of its π orbital with the π system of the phenyl ring and allows for the delocalization of the aromatic π electrons toward the sulfur atom through the conjugated system. A similar arrangement was seen in the cases of methyl phenyl sulfoxide (MPS)[8] and methyl 4-nitrophenyl sulfoxide (MNPSO).[9] Lacking sufficient isotopic information, the geometrical parameters for MPS and MNPSO were not well determined from the experiments. To make a consistent comparison, their structures were re-optimized at the same level of theory (B3LYP-D4/def2-QZVP), which was carried out for MTSO. The calculated rotational constants are in excellent agreement (with deviations of ~0.3%) with the

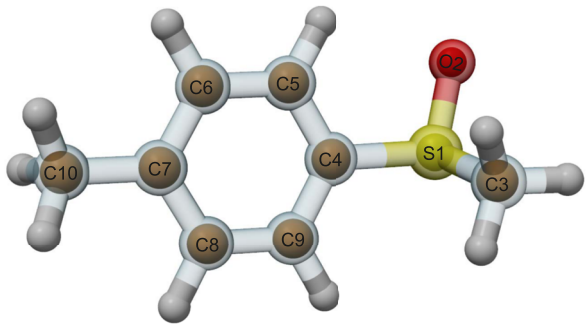

FIG. 4. Comparison of the calculated equilibrium structure (r_e, ball and stick model) of methyl *p*-tolyl sulfoxide (MTSO), obtained at the B3LYP-D4/def2-QZVP level of theory, with the experimentally determined heavy-atom positions (brown colored spheres: C, red colored spheres: O, and yellow colored spheres: S) in the effective ground state (r_0).

experimental results, as shown in Table S4. The optimized S=O/Ph dihedral angle is 6.0° and 3.1° for MPS and MNPSO, respectively. Considering that the methyl group is a weakly electron-donating group whereas the nitro-group (–NO_2) has a strong electron-withdrawing effect, it is likely that the S=O group tends to be subtly more twisted with respect to the phenyl plane when the *para*-substituent is more electron-donating.[10] Interestingly, the characteristic trigonal pyramidal geometry at the sulfur chiral center remains unaffected.

D. Excited state pyramidal inversion

Stereomutation at sulfur in chiral sulfoxides has widely been studied with both experimental and theoretical methods since the 1960s. The commonly accepted mechanism for the interconversion between the enantiomer pairs of aryl methyl sulfoxides is the pyramidal inversion.[42,43] Such inversion normally takes place under thermal (>200 °C) or chemical conditions (i.e., catalysts) and proceeds through a transition state where the pyramidal geometry at the sulfur becomes trigonal planar and achiral. The barrier to inversion is normally about 38–42 kcal/mol.[44] In this work, we re-investigated the sulfoxide inversion pathway for the three above-mentioned phenyl methyl sulfoxides using the NEB-transition state (TS) method (see Fig. S2 of the supplementary material). The transition states located on the potential pathway were optimized at the B3LYP-D4/def2-QZVP level of theory and confirmed with one imaginary frequency. The inversion barriers with zero-point energy (ZPE) corrections are predicted to be 41.9, 41.3, and 38.1 kcal/mol for MTSO, MPS, and MNPSO, respectively, which are in good agreement with previous studies.[43,45,46] The geometrical parameters involving sulfur are summarized in Table III. For each species, besides the trigonal planar geometry at the sulfur, the S–O bond length is elongated in the transition state, while both of the S–C bonds become shorter. In the case of MNPSO, the elongation of the S–O bond is less, whereas the contraction of the S–Ph bond is greater because of the electron-withdrawing effect of the *p*-NO_2 group. Furthermore, in comparison, the associated inversion barrier is lower in MNPSO.

When it comes to light-induced stereomutations, the inversion at the sulfur center in the photochemical environment is much faster than that in the electronic ground state.[47] Previous studies have ruled out the involvements of radical fragmentation and triplet states.[48] This implies that the barrier to pyramidal inversion in the electronic excited state is lower than the ground state barrier. An internal charge transfer (ICT) model for the excited state pyramidal inversion has been proposed by Kathayat *et al.*[10] A brief description is that the electron density at the sulfur center is reduced by charge transfer from the sulfoxide to the adjacent aromatic system after initial excitation to a locally excited state. The reduced electron density, mainly involving the sulfur lone pair, can cause less steric repulsion and, thus, lead to a lower barrier to the pyramidal inversion. The corresponding molecular orbital in MTSO, MPS, and MNPSO is the HOMO orbital, which includes the lone-pair character of the sulfur, as depicted in Fig. S3. The LUMO orbital, as a π^* orbital of the phenyl ring, is a candidate orbital to accept the electrons. Notably, the shape of the LUMO orbital is slightly shifted to the *para*-position in MNPSO due to the electron-withdrawing effect of the *p*-NO_2 group. This transition is found to take place in the $S_0 \rightarrow S_1$ excitation with a weight of ~95% for all three species. The vertical excitation energy in MNPSO (359 nm, oscillator strength (f_{osc}) = 0.084) is smaller than that in MTSO (266 nm, f_{osc} = 0.073) and MPS (268 nm, f_{osc} = 0.061). The pyramidal minimum energy

TABLE III. Geometrical parameters at the sulfur atom in the energetic minimum and transition state of MTSO, MPS, and MNPSO, respectively, in the electronic ground (S_0) and first excited (S_1) states, calculated at the TD-B3LYP/def2-QZVP level of theory.

	S_0 state			S_1 state		
	MTSO	MPS	MNPSO	MTSO	MPS	MNPSO
			Energetic minimum			
r(S–O) (Å)	1.486	1.486	1.483	1.490	1.487	1.475
r(S–Me) (Å)	1.821	1.821	1.821	1.803	1.801	1.793
r(S–Ph) (Å)	1.804	1.806	1.809	1.652	1.654	1.694
τ(Me–S–O–Ph) (deg)	109.4	109.4	109.6	127.5	127.7	128.0
τ(S=O/Ph)[a] (deg)	7.2	6.0	3.1	67.5	67.5	70.1
			Transition state			
ΔE[b] (kcal mol^{-1})	41.9	41.3	38.1	9.0	9.0	10.4
r(S–O) (Å)	1.505	1.503	1.494	1.493	1.490	1.474
r(S–Me) (Å)	1.787	1.788	1.788	1.796	1.796	1.796
r(S–Ph) (Å)	1.733	1.731	1.713	1.682	1.675	1.705
τ(Me–S–O–Ph) (deg)	180.0	180.0	180.0	179.7	179.0	179.3
τ(S=O/Ph)[a] (deg)	5.4	5.0	3.1	80.0	82.6	88.5

[a]Dihedral angle between the S=O group and the phenyl ring.
[b]Corrected with zero-point energies.

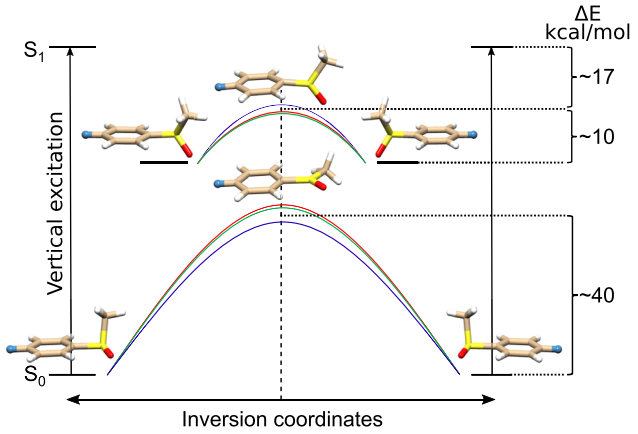

FIG. 5. Simple potential energetic pathways of the pyramidal inversion in the S_0 and S_1 states for MTSO (red curve), MPS (green curve), and MNPSO (blue curve), respectively, calculated at the TD-B3LYP/def2-QZVP level of theory. In order to highlight the inversion barrier heights, the energetic minima for all three species are set to the same level for S_0 and S_1, respectively. Displayed geometries correspond to the vibrational ground state and transition states at the inversion barrier. The light blue ball in each of the geometries represents the *para*-substituents, which are CH_3, H, and NO_2.

structure and the planar transition state for each molecule were optimized in the S_1 state, as shown in Fig. 5. Comparing the excited state with the ground state, as summarized in Table III, the sulfoxide group in the equilibrium structure is ~60° more twisted from the phenyl plane and the pyramidal geometry is ~20° closer to the trigonal planar. In the corresponding transition state, the sulfoxide group changes from a pyramidal to a planar arrangement. This planar sulfoxide group is oriented almost perpendicularly to the ring plane instead of being co-planar as in the electronic ground state. The energy barrier to the planar geometry is significantly reduced to 9.0, 9.0, and 10.4 kcal/mol for MTSO, MPS, and MNPSO, respectively, which reinforces the idea that the electron-withdrawing effect of a *para*-substituent (e.g., $-NO_2$) leads to a higher inversion barrier in the S_1 state.[10] In addition, we have calculated the energy of the S_1 state when it is excited in a vertical $S_0 \rightarrow S_1$ excitation. At this geometry, the potential is 17.9, 18.1, and 19.9 kcal/mol above the inversion barrier for MTSO, MPS, and MNPSO, respectively. Consequently, optical excitation to S_1 can lead to a rapid, non-thermal inversion of the handedness, which makes this molecule ideally suited to change and control its chirality using adapted light pulses.

V. SUMMARY

In summary, the rotational spectrum of methyl *p*-tolyl sulfoxide, where one conformer was unambiguously observed, was reported. By taking advantage of the assignments of the normal species and the ^{34}S and ^{13}C singly substituted isotopologues in their natural abundances, the effective ground state geometry (r_0) was readily determined, which is in good agreement with the equilibrium structure (r_e) obtained from the DFT calculation. As the methylsulfinyl group and the *p*-methyl group are situated at the opposite ends of the phenyl ring, the intramolecular interactions between them, including steric repulsions and dispersion attractions, are nearly negligible. Interestingly, the two functional groups can still interact with each other through the delocalized π system in the phenyl ring. On the one hand, the electronic effect of the methylsulfinyl group, which causes subtle changes in the π cloud, is sensitively probed by the internal rotation of the *p*-methyl group. The barrier of the internal rotation motion is determined to be only 11.0178(23) cm^{-1} from the observed *A*/*E* splittings of the rotational transitions, which is lower than that of many other similar *para*-substituted toluenes. The low barrier results from lower electron density around the methyl group and indicates an electron-withdrawing effect of the methylsulfinyl group. On the other hand, the *para*-substituents have clear impacts on the pyramidal inversion dynamics of the sulfoxide group in both the ground and first electronically excited states. With the TD-B3LYP calculations, it is, evidently, shown that the sulfoxide pyramidal inversion is significantly more facile in the S_1 state and, after vertical excitation to S_1 with optimized light pulses, the handedness is likely to interconvert barrierlessly.

SUPPLEMENTARY MATERIAL

See the supplementary material for further details of *A*/*E* splittings (Fig. S1), pyramidal inversion pathways (Fig. S2), HOMO–LUMO orbital contributions to the $S_0 \rightarrow S_1$ transitions (Fig. S3), complete results of the BELGI-C_1 and XIAM fits (Tables S1–S3), rotational constant deviations for MPS and MNPSO (Table S4), and experimental transition frequencies (Tables S5–S14).

ACKNOWLEDGMENTS

This research was supported by the Sonderforschungsbereich under Grant No. SFB 1319 "ELCH" of the Deutsche Forschungsgemeinschaft. The computational work was supported through the European XFEL and DESY funded Maxwell computational resources operated at Deutsches Elektronen-Synchrotron DESY, Hamburg, Germany.

AUTHOR DECLARATIONS

Conflict of Interest

The authors have no conflicts to disclose.

DATA AVAILABILITY

The data that support the findings of this study are available within the article and its supplementary material or from the corresponding authors upon reasonable request.

REFERENCES

[1] B. Långström and G. Bergson, "Asymmetric induction in a Michael-type reaction," Acta Chem. Scand. **27**, 3118–3119 (1973).
[2] S. F. Mason and G. E. Tranter, "The parity-violating energy difference between enantiomeric molecules," Chem. Phys. Lett. **94**, 34–37 (1983).
[3] S. R. Domingos, C. Pérez, and M. Schnell, "Communication: Structural locking mediated by a water wire: A high-resolution rotational spectroscopy study on hydrated forms of a chiral biphenyl derivative," J. Chem. Phys. **145**, 161103 (2016).

[4]J. Han, V. A. Soloshonok, K. D. Klika, J. Drabowicz, and A. Wzorek, "Chiral sulfoxides: Advances in asymmetric synthesis and problems with the accurate determination of the stereochemical outcome," Chem. Soc. Rev. **47**, 1307–1350 (2018).

[5]M. Quack and G. Seyfang, "Tunnelling and parity violation in chiral and achiral molecules: Theory and high-resolution spectroscopy," in *Tunnelling in Molecules* (Royal Society of Chemistry, 2020), pp. 192–244.

[6]D. Tikhonov, personal communication (2021).

[7]K. Fehre, S. Eckart, M. Kunitski, M. Pitzer, S. Zeller, C. Janke, D. Trabert, J. Rist, M. Weller, A. Hartung, L. P. H. Schmidt, T. Jahnke, R. Berger, R. Dörner, and M. S. Schöffler, "Enantioselective fragmentation of an achiral molecule in a strong laser field," Sci. Adv. **5**, eaau7923 (2019).

[8]G. Celebre, G. Cinacchi, G. De Luca, B. M. Giuliano, F. Iemma, and S. Melandri, "Multitechnique investigation of conformational features of small molecules: The case of methyl phenyl sulfoxide," J. Phys. Chem. B **112**, 2095–2101 (2008).

[9]G. Celebre, G. De Luca, M. E. Di Pietro, B. M. Giuliano, S. Melandri, and G. Cinacchi, "Detection of significant aprotic solvent effects on the conformational distribution of methyl 4-nitrophenyl sulfoxide: From gas-phase rotational to liquid-crystal NMR spectroscopy," ChemPhysChem **16**, 2327–2337 (2015).

[10]R. S. Kathayat, L. Yang, T. Sattasathuchana, L. Zoppi, K. K. Baldridge, A. Linden, and N. S. Finney, "On the origins of nonradiative excited state relaxation in aryl sulfoxides relevant to fluorescent chemosensing," J. Am. Chem. Soc. **138**, 15889–15895 (2016).

[11]K. Hoki, L. González, and Y. Fujimura, "Quantum control of molecular handedness in a randomly oriented racemic mixture using three polarization components of electric fields," J. Chem. Phys. **116**, 8799–8802 (2002).

[12]D. Gerbasi, M. Shapiro, and P. Brumer, "Theory of 'laser distillation' of enantiomers: Purification of a racemic mixture of randomly oriented dimethylallene in a collisional environment," J. Chem. Phys. **124**, 074315 (2006).

[13]W. Gordy, "Microwave spectroscopy," Rev. Mod. Phys. **20**, 668–717 (1948).

[14]W. Sun, O. P. Sogeke, W. G. D. P. Silva, and J. van Wijngaarden, "Dispersion-driven conformational preference in the gas phase: Microwave spectroscopic and theoretical study of allyl isocyanate," J. Chem. Phys. **151**, 194304 (2019).

[15]M. Fatima, C. Pérez, B. E. Arenas, M. Schnell, and A. L. Steber, "Benchmarking a new segmented K-band chirped-pulse microwave spectrometer and its application to the conformationally rich amino alcohol isoleucinol," Phys. Chem. Chem. Phys. **22**, 17042–17051 (2020).

[16]F. Neese, "The ORCA program system," Wiley Interdiscip. Rev.: Comput. Mol. Sci. **2**, 73–78 (2011).

[17]F. Neese, "Software update: The ORCA program system, version 4.0," Wiley Interdiscip. Rev.: Comput. Mol. Sci. **8**, e1327 (2018).

[18]A. D. Becke, "Density-functional exchange-energy approximation with correct asymptotic behavior," Phys. Rev. A **38**, 3098–3100 (1988).

[19]A. D. Becke, "Density-functional thermochemistry. III. The role of exact exchange," J. Chem. Phys. **98**, 5648–5652 (1993).

[20]P. J. Stephens, F. J. Devlin, C. F. Chabalowski, and M. J. Frisch, "Ab initio calculation of vibrational absorption and circular dichroism spectra using density functional force fields," J. Phys. Chem. Lett. **98**, 11623–11627 (1994).

[21]E. Caldeweyher, S. Ehlert, A. Hansen, H. Neugebauer, S. Spicher, C. Bannwarth, and S. Grimme, "A generally applicable atomic-charge dependent London dispersion correction," J. Chem. Phys. **150**, 154122 (2019).

[22]F. Weigend and R. Ahlrichs, "Balanced basis sets of split valence, triple zeta valence and quadruple zeta valence quality for H to Rn: Design and assessment of accuracy," Phys. Chem. Chem. Phys. **7**, 3297–3305 (2005).

[23]D. Bykov, T. Petrenko, R. Izsák, S. Kossmann, U. Becker, E. Valeev, and F. Neese, "Efficient implementation of the analytic second derivatives of Hartree–Fock and hybrid DFT energies: A detailed analysis of different approximations," Mol. Phys. **113**, 1961–1977 (2015).

[24]O.-P. Koistinen, F. B. Dagbjartsdóttir, V. Ásgeirsson, A. Vehtari, and H. Jónsson, "Nudged elastic band calculations accelerated with Gaussian process regression," J. Chem. Phys. **147**, 152720 (2017).

[25]R. Bauernschmitt and R. Ahlrichs, "Treatment of electronic excitations within the adiabatic approximation of time dependent density functional theory," Chem. Phys. Lett. **256**, 454–464 (1996).

[26]T. Lu and F. Chen, "Multiwfn: A multifunctional wavefunction analyzer," J. Comput. Chem. **33**, 580–592 (2012).

[27]H. M. Pickett, "The fitting and prediction of vibration-rotation spectra with spin interactions," J. Mol. Spectrosc. **148**, 371–377 (1991).

[28]J. K. G. Watson, "Determination of centrifugal distortion coefficients of asymmetric-top molecules," J. Chem. Phys. **46**, 1935–1949 (1967).

[29]H. Hartwig and H. Dreizler, "The microwave spectrum of trans-2,3-dimethyloxirane in torsional excited states," Z. Naturforsch., A **51**, 923–932 (1996).

[30]J. T. Hougen, I. Kleiner, and M. Godefroid, "Selection rules and intensity calculations for a C_s asymmetric top molecule containing a methyl group internal rotor," J. Mol. Spectrosc. **163**, 559–586 (1994).

[31]I. Kleiner and J. T. Hougen, "Rho-axis-method Hamiltonian for molecules having one methyl rotor and C_1 point-group symmetry at equilibrium," J. Chem. Phys. **119**, 5505–5509 (2003).

[32]U. de la Camp and H. Hope, "The crystal structure and absolute configuration of (+)-methyl-*p*-tolyl sulfoxide," Acta Crystallogr., Sect. B: Struct. Crystallogr. Cryst. Chem. **26**, 846–853 (1970).

[33]H. D. Rudolph and A. Trinkaus, "Mikrowellenspektrum, hinderungspotential der internen rotation und dipolmoment des meta-fluortoluols," Z. Naturforsch., A **23**, 68–76 (1968).

[34]A. Hellweg and C. Hättig, "On the internal rotations in *p*-cresol in its ground and first electronically excited states," J. Chem. Phys. **127**, 024307 (2007).

[35]S. Herbers, S. M. Fritz, P. Mishra, H. V. L. Nguyen, and T. S. Zwier, "Local and global approaches to treat the torsional barriers of 4-methylacetophenone using microwave spectroscopy," J. Chem. Phys. **152**, 074301 (2020).

[36]H. Saal, J.-U. Grabow, A. R. Hight Walker, J. T. Hougen, I. Kleiner, and W. Caminati, "Microwave study of internal rotation in para-tolualdehyde: Local versus global symmetry effects at the methyl-rotor site," J. Mol. Spectrosc. **351**, 55–61 (2018).

[37]L. Ferres, W. Stahl, I. Kleiner, and H. V. L. Nguyen, "The effect of internal rotation in *p*-methyl anisole studied by microwave spectroscopy," J. Mol. Spectrosc. **343**, 44–49 (2018).

[38]E. G. Schnitzler, N. A. Seifert, I. Kusuma, and W. Jäger, "Rotational spectroscopy of *p*-toluic acid and its 1:1 complex with water," J. Phys. Chem. A **121**, 8625–8631 (2017).

[39]A. H. Yateem, "Rotational barrier and electron-withdrawing substituent effects: Theoretical study of π-conjugation in para-substituted anilines," Mediterr. J. Chem. **10**, 319–334 (2020).

[40]D. R. Lima, S. Q. de Aguiar Filho, L. B. C. do Oh, A. K. Dos Santos Pereira, and D. H. Pereira, "Theoretical study of internal rotational barriers of electrons donating and electrons withdrawing groups in aromatic compounds," Heliyon **6**, e04957 (2020).

[41]R. Schwendeman, "Structural parameters from rotational spectra," in *Critical Evaluation of Chemical and Physical Structural Information* (National Academy of Sciences, Washington, DC, 1974).

[42]D. R. Rayner, E. G. Miller, P. Bickart, A. J. Gordon, and K. Mislow, "Mechanisms of thermal racemization of sulfoxides," J. Am. Chem. Soc. **88**, 3138–3139 (1966).

[43]H. Marom, P. U. Biedermann, and I. Agranat, "Pyramidal inversion mechanism of simple chiral and achiral sulfoxides: A theoretical study," Chirality **19**, 559–569 (2007).

[44]C. Aurisicchio, E. Baciocchi, M. F. Gerini, and O. Lanzalunga, "Thermal and photochemical racemization of chiral aromatic sulfoxides via the intermediacy of sulfoxide radical cations," Org. Lett. **9**, 1939–1942 (2007).

[45]D. R. Rayner, A. J. Gordon, and K. Mislow, "Thermal racemization of diaryl, alkyl aryl, and dialkyl sulfoxides by pyramidal inversion," J. Am. Chem. Soc. **90**, 4854–4860 (1968).

[46]D. Balcells, F. Maseras, and N. Khiar, "Base-catalyzed inversion of chiral sulfur centers. A computational study," Org. Lett. **6**, 2197–2200 (2004).

[47]Y. Guo and W. S. Jenks, "Photolysis of alkyl aryl sulfoxides: α-cleavage, hydrogen abstraction, and racemization," J. Org. Chem. **62**, 857–864 (1997).

[48]W. Lee and W. S. Jenks, "Photophysics and photostereomutation of aryl methyl sulfoxides," J. Org. Chem. **66**, 474–480 (2001).